

# Reliability of MRI-derived measurements of human cerebral cortical thickness: The effects of field strength, scanner upgrade and manufacturer

Xiao Han,<sup>a,b</sup> Jorge Jovicich,<sup>a,b</sup> David Salat,<sup>a,b</sup> Andre van der Kouwe,<sup>a,b</sup> Brian Quinn,<sup>a,b</sup> Silvester Czanner,<sup>a,b</sup> Evelina Busa,<sup>a,b</sup> Jenni Pacheco,<sup>a,b</sup> Marilyn Albert,<sup>d,e</sup> Ronald Killiany,<sup>f</sup> Paul Maguire,<sup>g</sup> Diana Rosas,<sup>a,b,c</sup> Nikos Makris,<sup>a,b,h</sup> Anders Dale,<sup>i</sup> Bradford Dickerson,<sup>a,c,d,j,l</sup> and Bruce Fischl<sup>a,b,k,\*,l</sup>

<sup>a</sup>Athinoula A. Martinos Center for Biomedical Imaging, Massachusetts General Hospital and Harvard Medical School, Boston, MA 02129, USA

<sup>b</sup>Department of Radiology, Massachusetts General Hospital and Harvard Medical School, Boston, MA 02129, USA

<sup>c</sup>Department of Neurology, Massachusetts General Hospital and Harvard Medical School, Boston, MA 02129, USA

<sup>d</sup>Gerontology Research Unit/Department of Psychiatry, Massachusetts General Hospital and Harvard Medical School, Boston, MA 02129, USA

<sup>e</sup>Department of Neurology, Johns Hopkins University School of Medicine, Baltimore, MD 21288, USA

<sup>f</sup>Department of Anatomy and Neurobiology, Boston University School of Medicine, Boston, MA 02215, USA

<sup>g</sup>Pfizer Global Research and Development, Groton, CT 06340, USA

<sup>h</sup>Center for Morphometric Analysis, Massachusetts General Hospital, Boston, MA 02129, USA

<sup>i</sup>University of California San Diego, CA 92093, USA

<sup>j</sup>Division of Cognitive and Behavioral Neurology, Department of Neurology, Brigham and Women's Hospital, Boston, MA 02115, USA

<sup>k</sup>CSAIL, MIT, Cambridge, MA 02142, USA

Received 21 October 2005; revised 17 February 2006; accepted 27 February 2006

Available online 2 May 2006

**In vivo MRI-derived measurements of human cerebral cortex thickness are providing novel insights into normal and abnormal neuroanatomy, but little is known about their reliability. We investigated how the reliability of cortical thickness measurements is affected by MRI instrument-related factors, including scanner field strength, manufacturer, upgrade and pulse sequence. Several data processing factors were also studied. Two test–retest data sets were analyzed: 1) 15 healthy older subjects scanned four times at 2-week intervals on three scanners; 2) 5 subjects scanned before and after a major scanner upgrade. Within-scanner variability of global cortical thickness measurements was <0.03 mm, and the point-wise standard deviation of measurement error was approximately 0.12 mm. Variability was 0.15 mm and 0.17 mm in average, respectively, for cross-scanner (Siemens/GE) and cross-field strength (1.5 T/3 T) comparisons. Scanner upgrade did not increase variability nor introduce bias. Measurements across field strength, however, were slightly biased (thicker at 3 T). The number of (single vs. multiple averaged) acquisitions had a negligible effect on reliability, but the use of a**

**different pulse sequence had a larger impact, as did different parameters employed in data processing. Sample size estimates indicate that regional cortical thickness difference of 0.2 mm between two different groups could be identified with as few as 7 subjects per group, and a difference of 0.1 mm could be detected with 26 subjects per group. These results demonstrate that MRI-derived cortical thickness measures are highly reliable when MRI instrument and data processing factors are controlled but that it is important to consider these factors in the design of multi-site or longitudinal studies, such as clinical drug trials.**

© 2006 Elsevier Inc. All rights reserved.

*Keywords:* Cortical thickness; Structural MRI; Cerebral cortex; Morphology

## Introduction

Techniques that enable the in vivo MRI-derived quantitative measurement of properties of the human cerebral cortex, such as thickness, are beginning to demonstrate important potential applications in basic and clinical neuroscience. Changes in the gray matter that makes up the cortical sheet are manifested in normal aging (Jack et al., 1997; Salat et al., 1999, 2004; Sowell et al., 2003, 2004), Alzheimer's disease (Dickerson et al., 2001;

\* Corresponding author. Department of Radiology, NMR Center, Massachusetts General Hospital, 149 Thirteenth Street, Rm. 2301, Charlestown, MA 02129, USA. Fax: +1 617 726 7422.

E-mail address: [fischl@nmr.mgh.harvard.edu](mailto:fischl@nmr.mgh.harvard.edu) (B. Fischl).

<sup>1</sup> These authors contributed equally to this work.

Available online on ScienceDirect ([www.sciencedirect.com](http://www.sciencedirect.com)).

Thompson et al., 2003; Lerch et al., 2005), Huntington's disease (Rosas et al., 2002), corticobasal degeneration (Boeve et al., 1999), amyotrophic lateral sclerosis (Kiernan and Hudson, 1994), multiple sclerosis (Sailer et al., *in press*) and schizophrenia (Thompson et al., 2001; Kuperberg et al., 2003; Narr et al., 2005). Progressive thinning of the cortex follows a disease-specific regional pattern in certain diseases, such as Alzheimer's disease (Thompson et al., 2003); thus, *in vivo* cortical thickness measures could be useful as a biomarker of the evolution of the disease. Longitudinal imaging-based biomarkers of disease progression will likely be of great utility in evaluating the efficacy of disease-modifying therapies (Dickerson and Sperling, 2005).

Measurement of cortical thickness from MRI data is a non-trivial task. Manual thickness measurements are difficult to obtain due to the highly convoluted nature of the cortex. It can take a trained anatomist several days to manually label a high-resolution set of MR brain images, and even this labor-intensive procedure allows only the measurement of cortical volume, not cortical thickness, because the cortical thickness is a property that can only be properly measured if the location and orientation of both the gray/white and pial surfaces are known. To facilitate automatic thickness measurement, many computerized methods have been proposed in the literature for segmenting the cortex and finding the cortical surfaces from MRI data (Dale et al., 1999; Joshi et al., 1999; MacDonald et al., 1999; Xu et al., 1999; Zeng et al., 1999; Van Essen et al., 2001; Shattuck and Leahy, 2002; Sowell et al., 2003; Barta et al., 2005; Han et al., 2005a).

Although the validation of MRI-derived cortical thickness measurements has been performed against regional manual measurements derived from both *in vivo* and post-mortem brain scans (Rosas et al., 2002; Kuperberg et al., 2003; Salat et al., 2004), the reliability of measures of this fundamental morphometric property of the brain has received relatively little systematic investigation (Fischl and Dale, 2000; Rosas et al., 2002; Kuperberg et al., 2003; Sowell et al., 2004; Lerch and Evans, 2005). Most of these studies approach reliability by comparing thickness measurements across different subjects or by performing repeated scans on a few subjects acquired within the same scan session or within very short scan intervals (for example, the subjects were removed from the scanner and then scanned again in 5 min (Sowell et al., 2004)). This approach may greatly underestimate the sources of variability within and between studies.

Variability in MRI-derived morphometric measures may result from subject-related factors, such as hydration status (Walters et al., 2001), instrument-related factors, such as field strength, scanner manufacturer or pulse sequence, or data-processing-related factors, including not only software package but also the parameters chosen for analysis. All of these factors may contribute to differences between typical cross-sectional studies (e.g., when interpreting differences between two studies of patients with Alzheimer's disease vs. controls scanned at a single time point on one scanner). Longitudinal studies of normal development, aging or disease progression face additional challenges associated with both subject-related factors as well as instrument-related factors (e.g., major scanner upgrades). For multi-site studies, it is critical to understand and adjust for instrument-related differences between sites, such as scanner manufacturer, field strength and other hardware components. Finally, longitudinal multi-center studies, such as the Alzheimer's Disease Neuroimaging Initiative, must contend with all of these factors while attempting to detect subtle effects. Thus, detailed quantitative data regarding the degree

to which each of the factors outlined above contribute to variability in cortical thickness (and other measures) could be very helpful for both study design and interpretation. Unfortunately, little work in this area has been performed.

Specifically, it is not yet clear how cortical thickness measures vary as a function of MRI instrument-related factors, such as field strength, scanner manufacturer and scanner software and hardware upgrades. Knowledge of the degree to which different MRI instrument-related factors affect the reliability of cortical thickness measures is essential for the interpretation of these measures in basic and clinical neuroscientific studies. Furthermore, this knowledge is critical if cortical thickness measures are to find applications as biomarkers in clinical trials of putative treatments for neurodegenerative or other neuropsychiatric diseases.

We undertook this study to evaluate the reliability of a cortical thickness measurement method both within and across different scanner platforms and field strengths, with the goal of quantitatively identifying the factors that are the greatest contributors to cortical thickness variability. Two groups of test–retest data sets were acquired and analyzed. In the first data set, 15 healthy older subjects were scanned four times at 2-week intervals on three different scanner platforms (test scan on Siemens Sonata 1.5 T, retest scan on Siemens Sonata 1.5 T, cross-site scan on GE Signa 1.5 T, cross-field-strength scan on Siemens Trio 3 T). Older participants were studied so that anatomical variability related to atrophy and age-related signal changes was represented. The 2-week interval was chosen so that elements of variability related to subject hydration status and minor instrument drift would be included, which may be artificially minimized when the test–retest interval is several min to ~1 day. First, the test–retest reliability of cortical thickness measurements was investigated from the two Siemens Sonata sessions. Next, analyses were performed on the effects of various instrument-related factors, including: a) different MR manufacturer (Siemens vs. GE); b) different field strength (1.5 T vs. 3 T); c) different pulse sequences (MPRAGE versus multiple flip angle, multi-echo FLASH); d) different number of data acquisitions (one MPRAGE vs. two averaged MPRAGE acquisitions). Finally, effects of several data processing-related factors were analyzed, including: a) different levels of spatial smoothing of the raw thickness maps; and b) different processing schemes (cross-sectional versus longitudinal).

The second data set consisted of 5 healthy younger subjects scanned repeatedly before and after a major scanner upgrade, with the goal of evaluating the reliability of thickness measurements in longitudinal studies that contend with scanner upgrades.

In this study, thickness measurements were performed using the FreeSurfer software package, which is an automated method for cortical surface reconstruction and thickness computation. Although comparison with other thickness measurement methods is beyond the scope of this paper, the effects of several aspects of the processing system within FreeSurfer were studied as noted above.

## Materials and methods

### Data acquisition

Two groups of test–retest data sets were acquired and analyzed to characterize the reliability of cortical thickness estimation.

The first group of test–retest data consists of MRI scans acquired from 15 healthy older subjects (age between 66 and 81 years; mean: 69.5 years; SD: 4.8 years. 8 males, 7 females). All participants provided informed consent in accordance with the Human Research Committee of Massachusetts General Hospital. Each subject underwent 4 scan sessions at 2-week intervals (two of the subjects were each missing one scan session), including two sessions on a Siemens 1.5 T Sonata scanner (Siemens Medical Solutions, Erlangen, Germany), one on a Siemens 3 T Trio scanner and one on a GE 1.5 T Signa scanner (General Electric, Milwaukee, WI).

For each Siemens scan session, the acquisition included two MPRAGE volumes (190 Hz/pixel, flip angle = 7°, 1.5 T: TR/TE/TI = 2.73 s/3.44 ms/1 s, 3 T: TR/TE/TI = 2.53 s/3.25 ms/1.1 s) and two multi-echo multi flip angle (30° and 5°) fast low-angle shot (FLASH) volumes (651 Hz/pixel, TR = 20 ms, TE = (1.8 + 1.82 \*  $n$ ) ms,  $n = 0, \dots, 7$ ; both for 1.5 T and 3 T). In each GE session, only the two MPRAGE volumes were acquired, but no multi-echo FLASH (MEF). Acquisition time for MPRAGE and MEF sequences was roughly the same and about 8 min each. All scans were 3D sagittal acquisitions with 128 contiguous slices (imaging matrix = 256 × 192, in-plane resolution = 1 mm, slice thickness = 1.33 mm). In each Siemens scan session, the acquisitions were automatically aligned to a standardized anatomical atlas to ensure consistent slice prescription across scans (Van der Kouwe et al., 2005; Benner et al., in press).

In the second group of test–retest data, 5 healthy volunteers (34 ± 3 years of age; 1 male, 4 females) were each scanned four times, twice before and twice after an MRI scanner upgrade (within 1 week for the repeated scans on the same scanner and the total time span was about 6 weeks). The upgrade was from a Siemens Magnetom Sonata to a Magnetom Avanto, which included the following major changes: a) main magnet (both are 1.5 T, Avanto's length is 150 cm, Sonata's is 160 cm), (b) gradient system (Avanto coils are more linear, Sonata 40 mT/m at 200 T/m/s, Avanto 45 mT/m at 200 T/m/s), c) head RF coil (circularly polarized on Sonata, 12 channels in Avanto) and d) software upgrade. During each of the four scan sessions, two MPRAGE volumes were acquired for each subject with the same sequence parameter settings as the MPRAGE scans in the first group. This second group of data is used to evaluate the thickness measurement reliability with respect to changes in scanner platform and also the measurement reliability before and after the scanner upgrade.

#### *Cortical surface reconstruction and cortical thickness measurement*

Reconstruction of the cortical surfaces was performed using the FreeSurfer toolkit (which is freely available to the research community through the website <http://www.surfer.nmr.mgh.harvard.edu>). This suite of methods was initially proposed in 1999 (Dale et al., 1999; Fischl et al., 1999a) and has undergone several important improvements over the years (Fischl et al., 1999b, 2001, 2002; Segonne et al., 2004). With these updates, the current method is fully automated. All the surface reconstruction results reported in this paper were generated using the fully automated processing pipeline, and no manual intervention was involved.

In FreeSurfer, when multiple acquisitions of the same pulse sequence are available for the same subject in each scan session, they are usually simply averaged after motion correction to generate a single volume with better signal-to-noise ratio (SNR)

(the effect of number of acquisitions on thickness measurement reliability is also investigated in this study). The multiple volumes from the MEF sequence, however, have very different contrast properties due to the different flip angle settings. Thus, a weighted average is adopted instead. The weighting coefficients (a unit vector of length 16) were pre-computed using a set of 11 MEF scans that have complete manual labeling for gray matter (GM) and white matter (WM). An optimal weighting was first computed for each data set based on the principle of linear discriminant analysis (Duda et al., 2001), with the objective to maximize the contrast-to-noise-ratio (CNR) between GM and WM. The weighting vectors from the 11 training data sets were then averaged to get the final weighting coefficients that are used for the processing of new MEF data.

Cortical thickness estimates in this study are computed as follows. For each point on the gray/white surface, the shortest distance to the pial surface is first computed. Next, for each point on the pial surface, the shortest distance to the gray/white surface is found, and the cortical thickness at that location is set to the average of these two values. Other thickness computation methods have been reported (Jones et al., 2000; Yezzi and Prince, 2003), but comparing their effects on the thickness reliability is outside the scope of this paper. We refer interested readers to Lerch and Evans (2005) for one such comparison.

#### *Evaluation of thickness measurement reliability*

Reliability (or reproducibility) of cortical thickness measurements was evaluated by comparing within subject thickness values between scan sessions. For example, using the within subject repeated MPRAGE scans from the first group of subjects, the measurement reliability can be evaluated either within the same scanner platform (using the two Sonata scans), or across different scanner platform (one Sonata and one Signa scan), or across different field strength (one Sonata and one Trio scan), or across both scanner platform and field strength (one Signa and one Trio scan).

In this study, both global and local thickness measurement reliability is evaluated, with the focus being on the latter. The global evaluation is performed by computing the global mean thickness value across the whole cortex for each subject and evaluating its reliability across difference scan sessions. To evaluate the error in local thickness measurements, surface point correspondence must be built to find thickness measurements at homologous cortical locations. The gray/white surface is used as reference to establish surface point correspondence since the gray/white surfaces are in general insensitive to atrophy, which could otherwise confound the alignment procedure.

Although each gray/white surface was mapped to the same surface atlas and their spherical coordinates can be used to find point correspondence between one surface and another, variations in the nonlinear surface registration or morphing often give rise to extra noise in the computed thickness difference or error map. Instead, a simpler linear registration is adopted to perform the intra-subject surface alignment, and surface point correspondence is then built according to their Euclidean distance in the registered space (typically, the maximal distance is less than 5 mm, and the mean and standard deviation of the absolute Euclidean distances are both less than 0.3 mm). The linear registration is computed using the FLIRT linear registration tool (Jenkinson et al., 2002). The volumetric registration matrix is then applied to the corresponding surfaces. It is found that, for registering surfaces across different

scan sessions of the same subject, the linear registration is sufficient and more robust than a nonlinear registration, which has an unnecessarily large number of degrees of freedom for this case. The nonlinear surface morphing is still necessary, however, in order to align thickness or thickness difference maps across different subjects for the computation of group-wise statistics. It should be noted that perfect surface node correspondence cannot be guaranteed and the computed thickness variability may include contributions from the surface registration error. Surface registration error, however, is unlikely to contribute significantly to the thickness variability measure, and its effect is further reduced if the raw thickness map is smoothed.

After the thickness difference maps have been computed for each subject and surface correspondence built across the group of subjects using the nonlinear surface morphing, the mean and standard deviation of the thickness differences can be computed at each location of the surface atlas over the group of subjects to evaluate the local thickness measurement variability. The relationship between the statistics of the thickness differences and the measurement variability (standard deviation of the measurement error) is worth some explanation. Assume that the measurement error can be modeled by a normal distribution  $N(0, \sigma_e^2)$  with zero mean (that is, unbiased) and standard deviation  $\sigma_e$ . Note that the standard deviation  $\sigma_e$  is a direct characterization of measurement variability that is often used in hypothesis testing and statistical power analysis. Given two measurements  $X$  and  $Y$  of the same thickness value  $\mu$  (e.g., from two repeated scans of the same subject), under the above assumption,  $X$  and  $Y$  both follow a normal distribution of  $N(\mu, \sigma_e^2)$ . From probability theory, their difference  $Z (= X - Y)$  follows a normal distribution of  $N(0, 2\sigma_e^2)$ . Clearly, given multiple observation of the difference  $Z$  at each homologous cortical location (each subject provides one such observation), its standard deviation  $\sigma_Z$  can be estimated, which in turn gives an estimate of the standard deviation of the measurement error according to the relationship  $\sigma_e = \sigma_Z / \sqrt{2}$ .

Another simpler statistic, used in this study, is the mean value of the absolute differences,  $E(|Z|)$ , computed at each surface atlas location. Through simple derivation, it can be obtained that  $E(|Z|) = 2\sigma_e / \sqrt{\pi} = 1.128\sigma_e$ . We chose  $E(|Z|)$  because it is more intuitive and can be interpreted as the mean measurement error and also because the estimation of means is more robust than the estimation of variance when sample sizes are small. We drop the factor of 1.128 when reporting the results, but keep in mind that it gives a slight overestimation of the measurement variability. In the Results section, maps of  $E(|Z|)$  will be presented to show the spatial pattern of measurement error. Note that, if the measurement noise is biased (i.e., having a non-zero mean  $\epsilon$ ),  $E(|Z|)$  is still a good approximation of  $\sigma_e$  as long as  $\epsilon \ll \sigma_e$ , but the overestimate is further increased.

#### *Effect of smoothing on thickness measurement reliability*

Note that, in the application of cortical thickness measurements for neuroscience studies, it is often necessary to perform spatial smoothing of the raw thickness maps (Fischl and Dale, 2000; Rosas et al., 2002; Kuperberg et al., 2003; Chung et al., 2005; Lerch and Evans, 2005; Narr et al., 2005). The smoothing reduces noise in the thickness measurements and increases the sensitivity and validity of statistical analysis (Chung et al., 2005; Lerch and Evans, 2005). The tradeoff is the reduction in the spatial resolution of the smoothed thickness maps. In this study, the effect of

different levels of spatial smoothing on the thickness reliability is also evaluated. The results can be used as a guide for users to choose the optimal smoothing when applying the thickness measurement method in practice.

Similar to a previous approach (Fischl and Dale, 2000), smoothing of the raw thickness maps is performed intrinsically on the surface tessellation using an iterative nearest-neighbor averaging procedure. At each iteration, the thickness value at a surface vertex is replaced by the average of the values at its immediate neighbors and at its own location. This procedure simulates the solution of a linear diffusion equation on the surface mesh and as such approximates a Gaussian smoothing kernel on the surface mesh. The total amount of smoothing is determined by the total number of iterations. A conservative approximation for the equivalent Gaussian kernel size is  $\sigma \leq \sqrt{N\Delta x}$ , where  $N$  is the number of iterations and  $\Delta x$  is the average vertex spacing. In the surface reconstruction results, a typical surface mesh contains about 120K vertices and the vertex spacing is less than 1 mm. From empirical simulation, it was found that  $N$  iterations of local averaging can be well approximated by a surface-based Gaussian filter of kernel size  $\sigma = \sqrt{2N/\pi}$ . This relationship is used throughout the presentation of the experimental results.

#### *Effect of number of acquisitions on thickness measurement reliability*

The MPRAGE scans from the first group of 15 subjects are used to study the effect of different number of image acquisitions on the thickness measurement reliability. For this purpose, cortical surface reconstruction and thickness measurement are also computed using only a single MPRAGE volume from each scan session. The thickness measurement reliability is then compared to the results when using the average of two MPRAGE volumes (which is the default approach).

#### *Effect of different processing schemes on thickness measurement reliability*

The surface reconstruction and thickness estimation procedure described above was designed for the processing of individual scans, and it is thus not optimal for the processing of longitudinal data (scans obtained at multiple time points from each subject). We also designed a longitudinal processing scheme that aims to incorporate the subject-wise correlation of longitudinal data into the processing stream in order to further reduce the measurement noise. Its performance in thickness measurement reliability is also evaluated and compared to the original cross-sectional method.

The longitudinal scheme differs from the original procedure in three major steps: preprocessing, intensity normalization and surface deformation. Assuming that a series of scans of the same subject are obtained at different time points, the data from time point one is first processed using the original procedure. For the processing of later time points, the three major steps mentioned above are modified. First, a linear registration is computed between the image volume of a later time point and that of the first time point. Note that the volume itself is not transformed, but only the registration matrix is stored and will be used in later steps. Second, at the intensity normalization step, instead of re-computing the WM control points, the control points (automatically computed) from time point one are mapped to the current volume using the previously computed linear registration, which are then used to

estimate the bias field. Third, at the surface deformation step, instead of starting the deformation from the topology-corrected WM tessellation, the gray/white and pial surfaces reconstructed from time point one are first transformed using the linear registration and then used to initialize the deformation for the gray/white and pial surfaces respectively for the current time point. Such an initialization scheme reduces the problem of deformable model methods being sensitive to initialization and local optimality (Dale et al., 1999; Xu et al., 1999; Han et al., 2005a). It also eliminates variation in initial surface tessellation and topology correction since these two steps are no longer needed in the processing of later time points. The performance of this method is evaluated in this study by considering the repeated scans from the different scan sessions as a longitudinal time series. It is noted that scripts for performing the longitudinal analysis are not included in the current distribution of FreeSurfer, but they will be made available to the public very soon.

#### *Effect of different imaging sequences on thickness measurement reliability*

In this comparison, cortical thickness measurements are computed using the MEF scans for the first group of 15 subjects, and the measurement reliability is compared with that of the MPRAGE scans. As explained earlier, the two MEF acquisitions from each scan session have different image contrast due to the different flip angle used, and thus a weighted average is applied to combine them into one single volume, which is then used as input for the cortical surface reconstruction and cortical thickness measurement. Since the MEF scans were not acquired on the GE scanner, the reliability of thickness from the MEF sequence data is only evaluated for the Siemens platform, both within and across field strengths.

#### *Reliability of thickness measurement with respect to scanner upgrade*

The second group of test–retest data is used to study the effect of scanner upgrade on thickness measurement reliability. For this purpose, thickness maps are first generated using data from each individual scan session of the 5 subjects (using the original cross-sectional scheme). Thickness difference maps are then computed between each pair of scans of the same subject. In particular, the pair of repeated scans before the scanner upgrade are used to estimate the measurement reliability on the old scanner platform and the other two for estimating the measurement reliability after the scanner upgrade. A third pair is formed by choosing one scan before the scanner upgrade and one afterward in order to evaluate the thickness reliability with respect to the upgrade. The thickness difference maps are all mapped to the common surface template, and their statistics (mean of the absolute thickness differences) are then computed over the group of subjects in order to estimate the measurement variability.

#### *Power analysis*

Given an estimation of the measurement error standard deviation, power calculations can be conducted to help answer questions such as how many subjects or samples are needed in order to detect a thickness change of a certain number of millimeters. This type of sample size determination is an important

step in planning a statistical study or clinical trial. The sample size is in general determined by the chosen significance level (the probability of type I error), desired statistical power (one minus the probability of type II error), the effect size and the standard deviation of measurement error (Cohen, 1988). There are no closed-form formulae for sample size determination, and the computation is usually done iteratively or using a look-up table.

In the Results section, sample size estimates results are presented based on the estimated thickness measurement variability. The first calculation was performed to estimate the sample size of detecting between-group differences between a group of patients with Alzheimer's disease (AD) and a group of controls. One estimate of the effect size for this type of study is 10%, based on data comparing mean cortical thickness between AD patients and controls (Thompson et al., 2003). Variability measures were derived from the cross-sectional cortical thickness analysis approach described above. A sample size estimate for a hypothetical clinical trial of a putative disease-modifying therapy for Alzheimer's disease was also performed. For this calculation, data from Thompson et al. (2003) were used to estimate the annual rate of cortical thinning in AD at 5% and in normal aging at 1%. In addition, a 50% treatment effect for a 1-year clinical drug trial was assumed, as was done by Jack et al. (2003). Thus, the effect size used in this calculation was 50% of the difference in the atrophy rates between the groups or  $0.5 \times 4\%/year = 2\%/year$ . For this calculation, variability measures were derived from the longitudinal cortical thickness analysis approach described above. For all sample size estimates, a significance level of 0.05 (one-sided) and a statistical power of 0.9 were assumed. The computation was performed using the standard formula as implemented in an online Java software algorithm developed by David A. Schoenfeld at our institute ([http://www.hedwig.mgh.harvard.edu/sample\\_size/size.html](http://www.hedwig.mgh.harvard.edu/sample_size/size.html)).

## Results and discussion

### *Reliability of global cortical thickness measure*

Global thickness measures for each subject are presented in Table 1, where the mean and standard deviation were computed

Table 1

Global thickness statistics (mean  $\pm$  SD) for each individual subject as measured using data from each scan session (in mm)

Subjects	Siemens 1.5 T	Siemens 1.5 T	GE 1.5 T	Siemens 3 T
1	2.06 $\pm$ 0.79	2.06 $\pm$ 0.78	2.05 $\pm$ 0.78	2.17 $\pm$ 0.81
2	2.12 $\pm$ 0.74	2.09 $\pm$ 0.75	2.13 $\pm$ 0.76	2.26 $\pm$ 0.78
3	2.03 $\pm$ 0.71	2.07 $\pm$ 0.71	2.07 $\pm$ 0.73	2.17 $\pm$ 0.73
4	2.00 $\pm$ 0.71	1.98 $\pm$ 0.71	1.98 $\pm$ 0.72	2.07 $\pm$ 0.75
5	1.93 $\pm$ 0.66	1.95 $\pm$ 0.68	1.94 $\pm$ 0.70	2.06 $\pm$ 0.71
6	1.79 $\pm$ 0.68	1.81 $\pm$ 0.68	1.83 $\pm$ 0.68	1.90 $\pm$ 0.69
7	2.15 $\pm$ 0.75	2.11 $\pm$ 0.74	2.12 $\pm$ 0.74	2.19 $\pm$ 0.76
8	1.98 $\pm$ 0.72	1.95 $\pm$ 0.73	1.98 $\pm$ 0.75	2.08 $\pm$ 0.77
9	2.02 $\pm$ 0.74	2.05 $\pm$ 0.76	2.08 $\pm$ 0.76	2.18 $\pm$ 0.79
10	1.91 $\pm$ 0.71	1.95 $\pm$ 0.68	1.94 $\pm$ 0.74	2.01 $\pm$ 0.75
11	1.96 $\pm$ 0.70	1.99 $\pm$ 0.71	1.96 $\pm$ 0.71	—
12	1.97 $\pm$ 0.70	1.99 $\pm$ 0.70	—	2.10 $\pm$ 0.72
13	2.08 $\pm$ 0.78	2.05 $\pm$ 0.78	2.12 $\pm$ 0.77	2.21 $\pm$ 0.79
14	1.93 $\pm$ 0.71	1.87 $\pm$ 0.70	1.96 $\pm$ 0.72	1.98 $\pm$ 0.73
15	1.82 $\pm$ 0.67	1.83 $\pm$ 0.67	1.79 $\pm$ 0.68	1.91 $\pm$ 0.70

“—” indicates two data sets not acquired.

over the whole cortical surface combining left and right hemispheres. Overall, the range of cortical thickness values is similar for each individual subject across different scan sessions. The reproducibility of global mean cortical thickness is further demonstrated in Fig. 1 for the four test–retest comparisons. As can be seen, the global mean thickness is an exceedingly reliable measure and highly reproducible across scan sessions. On average, the absolute difference in global mean cortical thickness is less than 0.03 mm within the same scanner platform. The mean absolute difference stays roughly the same even when comparing across different scanner platforms (i.e., Siemens Sonata vs. GE Signa). The variability is increased when comparing across field strengths but is still within 0.12 mm or about 1/8th of the voxel size on average. It is noted that the global mean thickness value is not affected by the degree of linear smoothing applied to the raw thickness maps, and thus the reproducibility of global mean thickness is independent of the level of smoothing.

The results in Fig. 1 also show that field strength has a larger effect on the reproducibility of mean cortical thickness than scanner platform, which is observed in all other thickness comparisons that were studied as well. As shown in the last column of Table 1, mean thickness values are slightly higher at 3 T than at 1.5 T. This effect is largely due to the fact that the underlying tissue NMR parameters and, in particular, the longitudinal relaxation time T1, change with field strength, which leads to changes in the intensity and contrast of the images. As a result, thickness measurements are biased across different field strengths, which contributes to the larger difference in global mean thickness when comparisons of 1.5 T and 3 T data are made. Note that this effect could be reduced by explicitly deriving sequences that minimize the contrast differences across field strength. Further study is required to determine which field strength gives thickness measurements that are more consistent with histological results.

#### Reliability of local cortical thickness measurement

To assess the local variability of cortical thickness measurement, the group-wise mean (in absolute value) of the thickness differences was computed at every location of the surface atlas, as described in the Materials and methods section. The thickness estimates were computed using the average of two MPRAGE

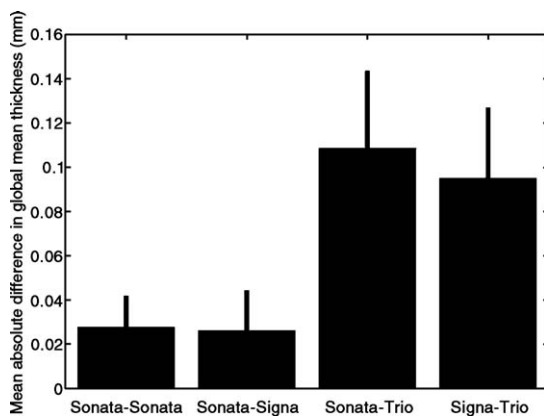


Fig. 1. Reproducibility of global mean cortical thickness across sites. The bar plots show the average absolute difference in global mean cortical thickness between pairs of repeated scans, and the error bars indicate one standard deviation. The names indicate scanner platform: Sonata, Siemens 1.5 T; Trio, Siemens 3 T; and Signa, GE 1.5 T.

volumes. Fig. 2 shows the maps for the local measurement variability, i.e., maps of the mean absolute thickness difference ( $E|Z|$  in the Materials and methods section) for the four test–retest comparisons, where a small surface-based blurring kernel (kernel size  $\sigma = 6$  mm) was used to smooth the raw thickness maps before the differences were computed (the effect of different smoothing level will be presented in the next section). Only the left hemisphere is shown; the right hemisphere is similar. Note that non-cortical regions were excluded in the computation using a mask that was initially drawn on the surface atlas and then mapped to each subject's surface, as indicated by the gray areas. The mask was drawn based on the surface curvature map and the surface parcellation scheme of Fischl et al. (2004b). It is intended to exclude non-cortical areas of the surface including the medial wall and the corpus callosum.

As shown in Fig. 2, the measurement variability (the average absolute thickness difference) is less than 0.12 mm for the bulk of the cortex when comparing thickness measurements within the same scanner platform. The average absolute difference value is slightly increased when comparing across platform or field strength but is still less than 0.15 mm for the majority of the cortex when platform but not field strength differs and less than 0.2 mm when field strength differs. The thickness measurement variability can be further reduced if a larger smoothing kernel is applied, as will be demonstrated in the next experiment. Note that the smoothing kernel size used here (6 mm) is very conservative when compared to what has been suggested in the literature as an optimal smoothing kernel, such as for example 30 mm (Chung et al., 2005; Lerch and Evans, 2005).

It is also clear from the maps in Fig. 2 that the thickness measurement variability is non-uniform across the cortex. The most variable area that is consistent across all the comparisons is a region around the precentral gyrus, which we believe reflects the local cytoarchitecture of this region of primary motor cortex. In particular, the special cytoarchitecture in this region leads to reduced gray/white contrast in T1-weighted images (Steen et al., 2000). Other areas with low gray/white contrast due to high degree of myelination, such as primary visual areas (Braitenberg and Schuz, 1991), also show larger measurement variability. To improve the reliability and accuracy of cortical estimations over the entire brain, it may thus be necessary to design new pulse sequences to achieve sufficient contrast in these regions.

There are some other regions that show higher levels of variability due to difficulties in the surface reconstruction. For example, the presence of dura tangential to the cortex and the close proximity of the two hemispheres often cause errors in localizing the pial surface in the medial frontal and anterior temporal regions and lead to larger thickness measurement variability. The narrow separation between putamen or hippocampus and the adjacent cortical gray matter also causes a problem in finding the gray/white surface around the insular and entorhinal cortex regions and also increases the thickness variability.

#### Effect of smoothing on thickness measurement reliability

Smoothing of raw thickness maps can reduce noise in the thickness measurements and thus improve reliability. To quantify the effect of smoothing on thickness reproducibility, different levels of smoothing were applied to the raw thickness map before computing the thickness differences and their statistics. Instead of showing all the measurement error maps as in Fig. 2, the results

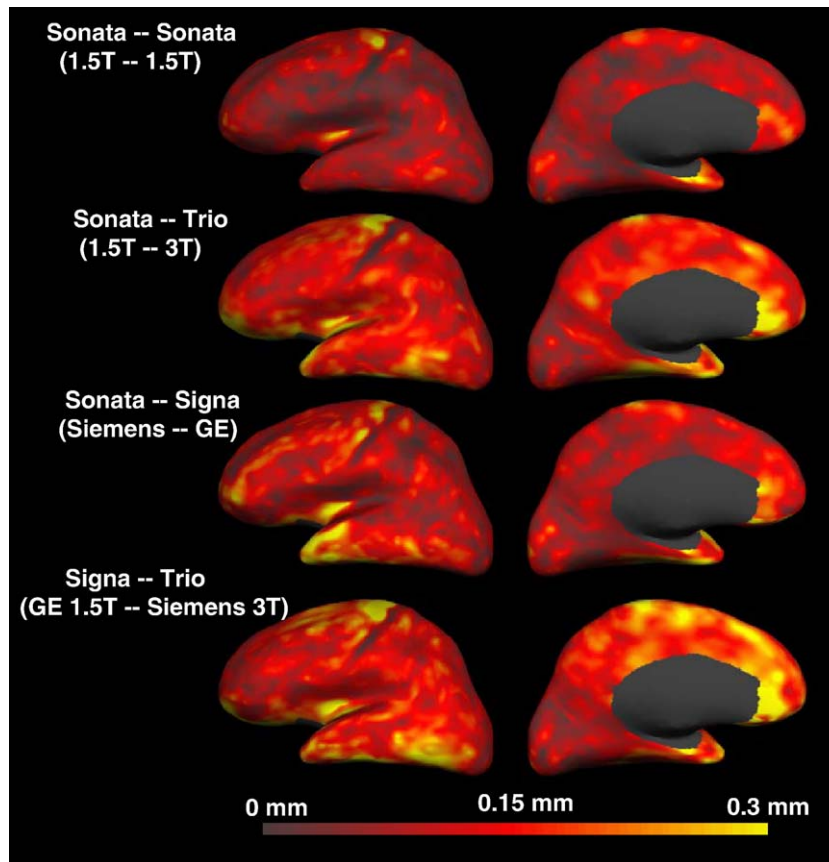


Fig. 2. Maps of thickness measurement variability for four test–retest comparisons (the left hemisphere only; the right hemisphere is similar). Subcortical regions and corpus callosum area are masked out since thickness is not defined there. The measurement variability is less than 0.12 mm for most the cortex for the within-scanner test–retest comparison and less than 0.2 mm for across platform comparisons. Left column: lateral view; right column: medial view.

were summarized by computing the overall mean of the thickness measurement error over each hemisphere of the surface atlas (masked areas being excluded), and these statistics were plotted as a function of the size of the smoothing kernel. The results are shown in Fig. 3.

These figures illustrate the observation that the thickness measurement variability becomes smaller as smoothing level increases (mean difference and standard deviation both become smaller). The rate of reduction of variability is high initially with

increasing blurring kernel size but slows with further increment of smoothing, which indicates that the autocorrelation of the measurement noise falls off rapidly with distance on the surface. Thus, it is sufficient to use a small kernel size to improve the reliability of the thickness comparisons without sacrificing much of the spatial resolution. As shown in Fig. 3, with a small smoothing kernel of 6 mm (much smaller than typically applied in the literature), the average error in thickness measurements with the same scanner is reduced to about 0.12 mm and is about 0.15 mm

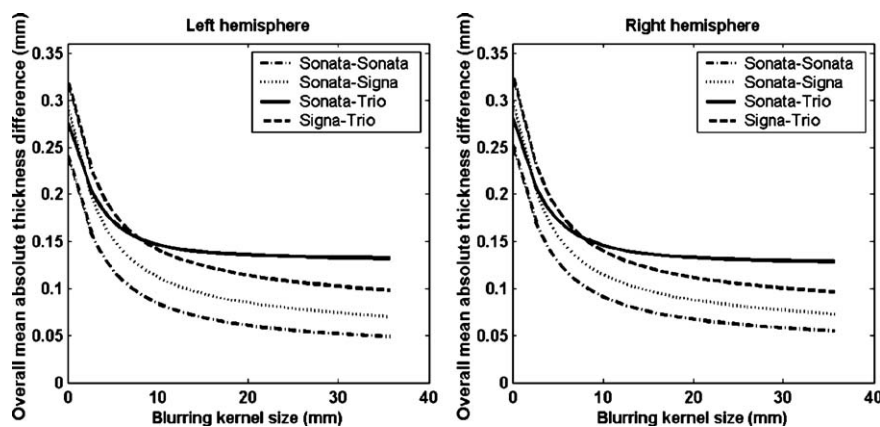


Fig. 3. Effects of smoothing on thickness measurement reproducibility. The plots show the overall mean of the absolute thickness difference map plotted as a function of smoothing kernel size. Left column: left hemisphere; right column, right hemisphere.

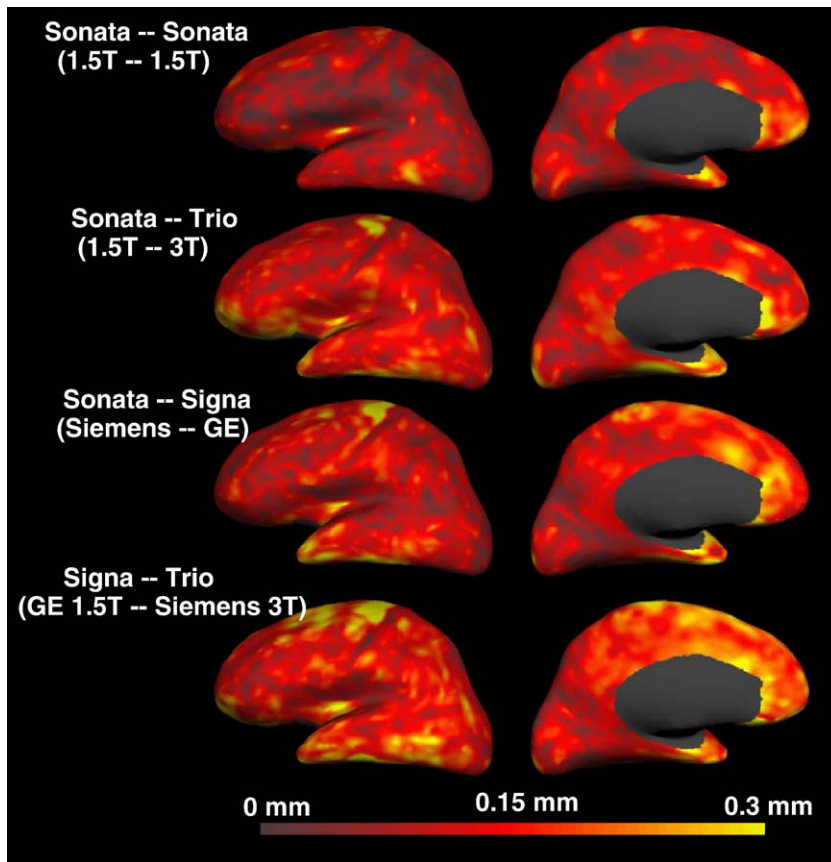


Fig. 4. Maps of thickness measurement variability for four test–retest comparisons using single MPRAGE acquisition. Left column: lateral view; right column: medial view. Only the left hemisphere is shown here; the right hemisphere is similar. A smoothing kernel of size  $\sigma = 6$  mm was applied when generating the thickness difference maps.

for cross platform and 0.17 mm for cross-field strength comparisons. With further increased smoothing (e.g., a size of 30 mm), the average within-scanner measurement error is only about 0.05 mm or 1/20th of the voxel size. Note that, when the kernel size is increased to infinity, the thickness at every surface location will be equal to the global mean and the differences reduce to the difference in the global means discussed in Fig. 1.

*Effect of number of acquisitions on thickness measurement reliability*

The above experiments used the average of two MPRAGE scans for the cortical thickness measurement. In this experiment, only a single MPRAGE acquisition is used (the first scan volume from each scan session was chosen for all subjects except one in

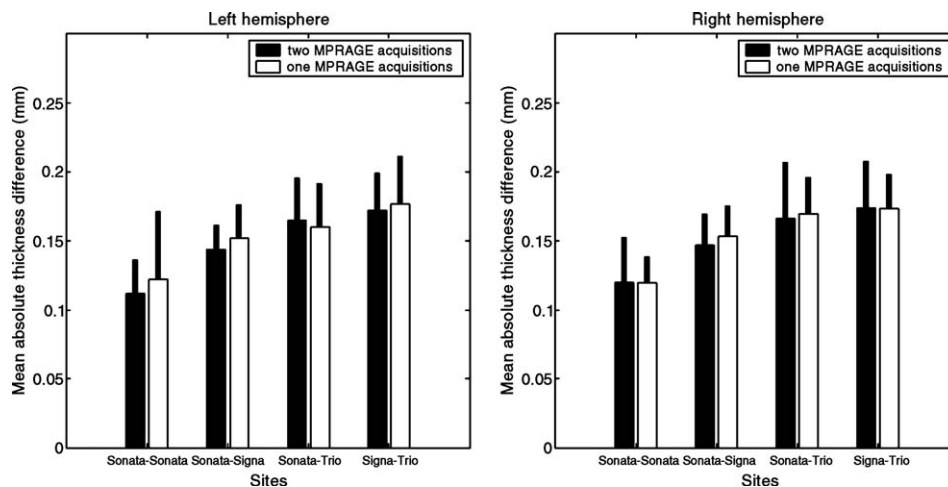


Fig. 5. Comparison of method reliability with one or two MPRAGE acquisitions. The bar plots show the overall mean thickness variability, and the error bars indicate one standard deviation. Left: left hemisphere; right: right hemisphere. A smoothing kernel of size  $\sigma = 6$  mm was applied.



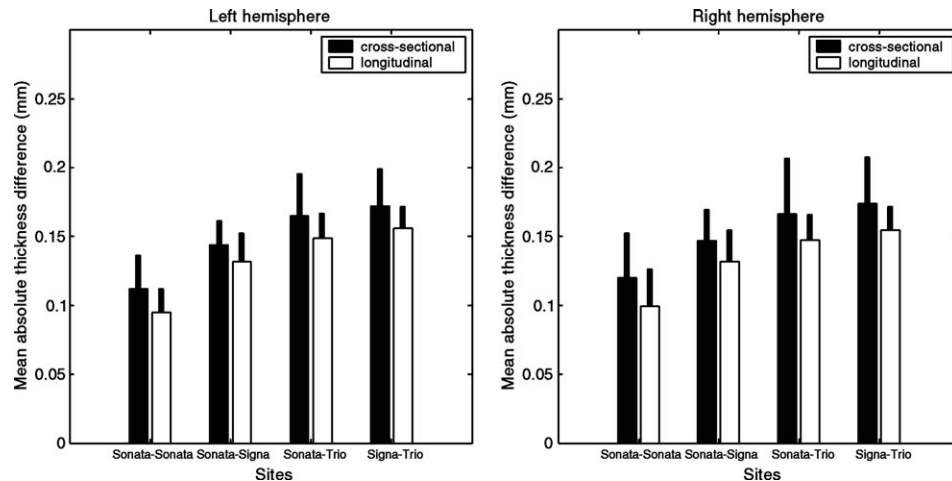


Fig. 6. Comparison of thickness measurement reliability using the cross-sectional and longitudinal processing schemes. The bar plots show the overall mean thickness variability, and the error bars indicate one standard deviation. Left: left hemisphere; right: right hemisphere. A smoothing kernel of size  $\sigma = 6$  mm was applied.

whom the first scan had obvious motion artifact; the second volume from this session was used instead). The resulting thickness measurement variability is compared against the case when using the average of both scans. The results are illustrated in Figs. 4 and 5, where Fig. 4 shows the maps of local thickness measurement variability for the four test–retest comparisons (left hemisphere only; the right hemisphere is similar) and Fig. 5

compares the overall mean of the measurement error. For this experiment, the surface smoothing kernel is fixed at 6 mm. Comparing Fig. 4 with Fig. 2, and from Fig. 5, it is clear that FreeSurfer performs almost as well on a single acquisition as on the average of two acquisitions.

The results appear surprising at first glance since averaging two acquisitions can improve the image SNR by a factor of square root

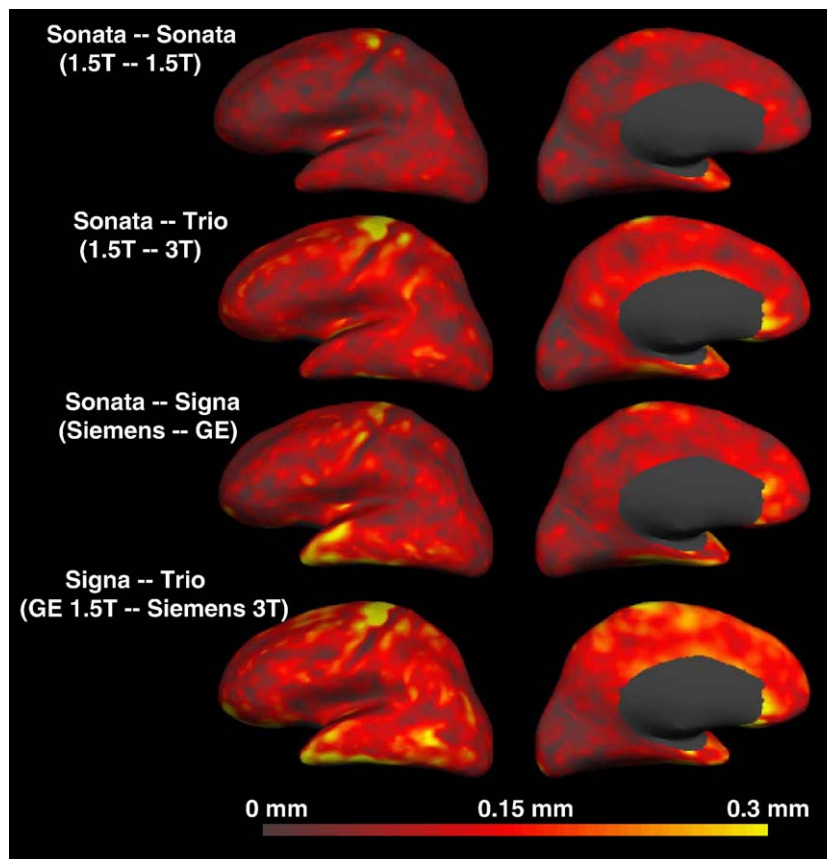


Fig. 7. Maps of thickness measurement variability for the longitudinal processing scheme (the left hemisphere only; the right hemisphere is similar). A smoothing kernel of size  $\sigma = 6$  mm was applied when generating the thickness difference maps.

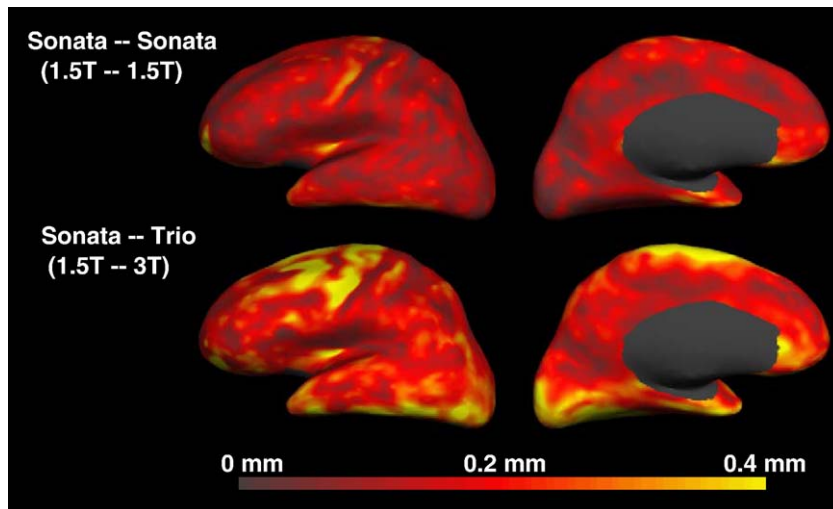


Fig. 8. Maps of thickness measurement variability with the MEF sequence (the left hemisphere only; the right hemisphere is similar). Left, lateral view; right: medial view. Note that the color scale used here is slightly different than in Fig. 2. A smoothing kernel of size  $\sigma = 6$  mm was applied when generating the thickness difference maps.

of 2, which could be expected to have a significant effect on the reproducibility of image segmentation. However, it should be noted that, when discriminating between two or more tissue classes like in cortical segmentation, it is the contrast-to-noise ratio (CNR) between tissue classes that matters. The “noise” in the term CNR refers to intensity variations within each tissue class, which not only includes background imaging noise, but also comprises intensity variations caused either by intrinsic tissue parameter variation across the brain or other imaging artifacts such as intensity non-uniformity and partial volume effects. Averaging multiple scans can only reduce background noise, but not the other sources of intensity variations. With current scanner technology (as for the scanners used in this study), background noise in a single-acquisition 1 mm MPRAGE scan is usually rather low and is certainly not the dominant factor for determining the segmentation accuracy or reliability. We observed that normal intensity variation within a tissue class (such as white matter) can be two or three times larger than the standard deviation of noise in the background. In addition, we found that it is difficult to obtain a perfect alignment between multiple acquisitions, and the averaged image

volume typically appears to be more blurred than individual scans, which leads to increased error in boundary estimation and variation in thickness measurements. All these factors should be taken into account when designing image acquisition and data processing. Note that, for subject populations for which movement is likely (e.g., pediatric or cognitively impaired subjects), acquiring multiple scans may always be desirable to ensure that there is at least one good scan to use for data analysis. Note also that the comparison results reported here may not be obtainable for data acquired at old scanners or be generalized to high-resolution scans (resolution  $< 1$  mm) where imaging noise in a single acquisition scan is still significant.

#### *Effect of the data processing scheme on thickness measurement reliability*

Fig. 6 compares the reliability of the longitudinal processing scheme against the cross-sectional one in thickness measurement. The two MPRAGE acquisitions in each scan session were used as inputs to the processing pipeline. The surface reconstruction results

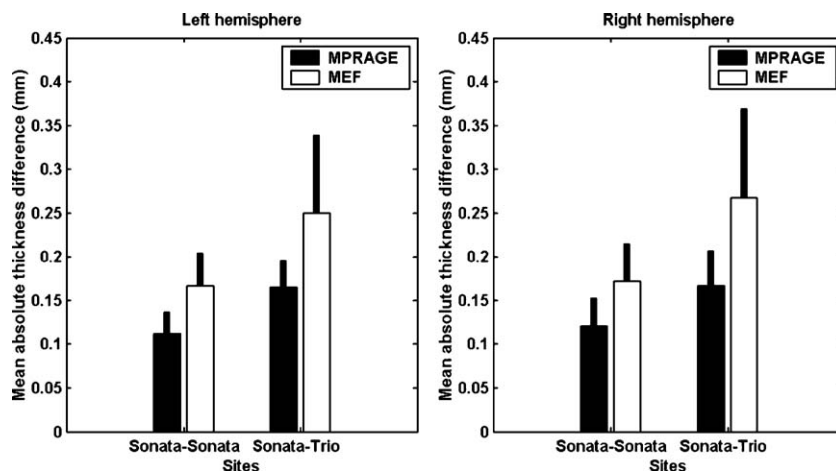


Fig. 9. Comparison of thickness measurement reliability with the MPRAGE and MEF sequences. The bar plots show the overall mean thickness variability, and the error bars indicate one standard deviation. Left: left hemisphere; right: right hemisphere. A smoothing kernel of size  $\sigma = 6$  mm was applied.

from the first scan session of each subject were used as initialization for the processing of later scans as described in the Materials and methods section. From the overall mean thickness measurement error, it is clear that the longitudinal processing scheme can further reduce the variability of the thickness measurements. The improvement due to the longitudinal method was found to be statistically significant at the significance level of 0.05 for all cases using paired  $t$  tests. Fig. 7 further shows the detailed maps of local thickness measurement error for the four comparisons. In the within-scanner test–retest case, the longitudinal scheme reduces the measurement variation to be lower than 0.09 mm for most of the cortex.

It should be noted that only the thickness measurement reliability is evaluated in this study. It is possible that errors in the surface reconstruction of an early time point might be propagated to a later time point with the longitudinal scheme, thus adversely affecting the accuracy of the later time point. Evaluating the effect of the longitudinal method on thickness accuracy is outside the scope of this paper but is worthy of further investigation.

#### *Effect of different imaging sequence on thickness measurement reliability*

In this experiment, the thickness measurement reliability was evaluated using the MEF scans acquired on the Siemens scanners. The local thickness measurement error maps are shown in Fig. 8 and Fig. 9 summarizes their overall mean and standard deviation. As Fig. 9 indicates, the average measurement error is less than 0.25 mm for both the within and across field strength comparisons (no cross-platform comparisons are available since MEF data were not acquired on the GE scanner).

Fig. 9 shows that the thickness reliability is poorer when using the MEF sequence than when using the MPRAGE. Fig. 10 helps explain the reason, where corresponding slices from an averaged MPRAGE volume and an averaged MEF volume from the same subject are shown side by side. Note that for the MEF volume a weighted averaging was used to achieve optimal gray/white contrast, as explained in the Materials and methods section. From the images, it is clear that MPRAGE gives better gray/white contrast than MEF (the average MEF image appears also more blurred, largely due to imperfect registration between the two individual acquisitions of different flip angles); this effect is

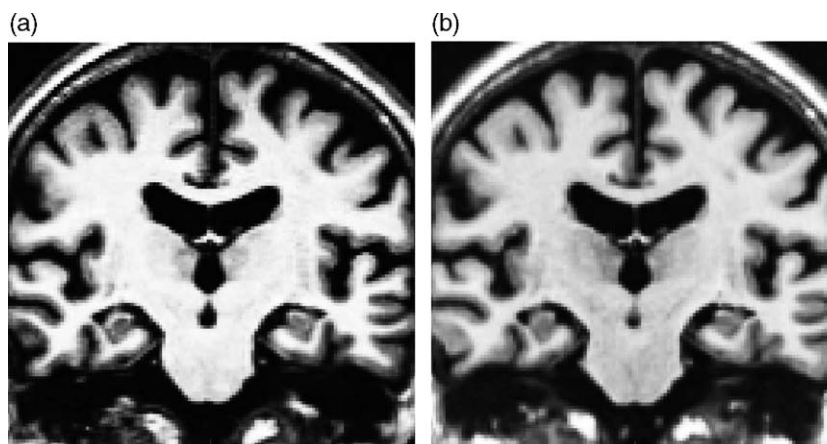


Fig. 10. Visual comparison of (a) MPRAGE and (b) MEF images: the MPRAGE image provides better gray/white CNR than the MEF image.

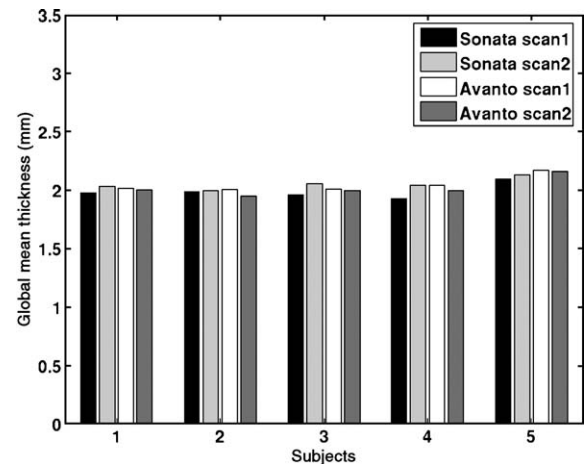


Fig. 11. Global mean cortical thickness of 5 subjects as measured from each of four repeated scans, including two before the scanner upgrade (Sonata) and two afterwards (Avanto). The global mean thickness measure is highly repeatable, and there is no noticeable bias due to scanner upgrade.

consistently seen in all other subjects' data as well. In a related study (Han et al., 2005b), we compared the CNR of the MPRAGE and MEF sequences (and also a single echo FLASH) using a set of manually labeled data. It was found that, even in the native space of original echos, MEF scans still have lower gray/white CNR (as measured by the Mahalanobis distance between the two tissue classes) than MPRAGE, although CNR for subcortical structures is higher. Thus, although the MEF sequence provides the advantage of allowing tissue parameter estimation (Fischl et al., 2004a), MPRAGE is currently a better sequence for studying morphometric changes in the cortical ribbon. Nonetheless, work is ongoing to further improve the segmentation of MEF data, including the investigation of better registration across different flip angles, and segmentation in the original multi-spectral space.

#### *Effect of scanner upgrade on thickness measurement reliability*

In this experiment, cortical thickness maps were generated from each of the four scans of the 5 subjects in the second group of test–retest data. Note that the four scans for each subject consist of two repeated scans before the scanner upgrade (Siemens Sonata) and two after the scanner upgrade (Siemens Avanto). Fig. 11 plots the

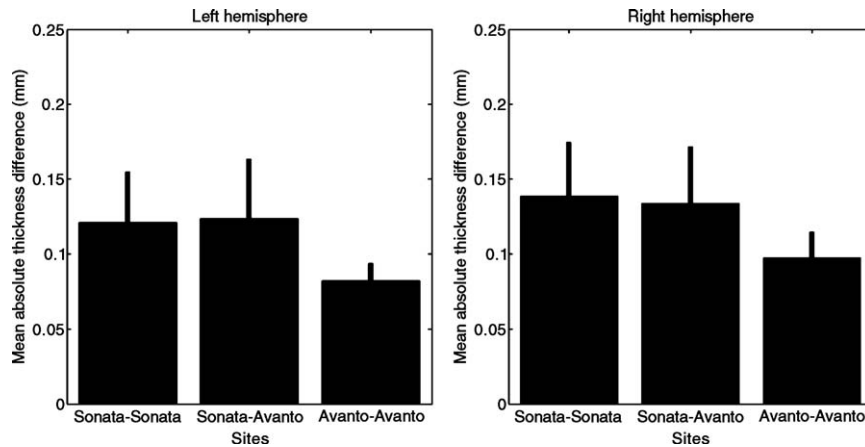


Fig. 12. Mean and standard deviation of thickness measurement variability before and after the scanner upgrade and variability between measurements across the scanner upgrade. The bar plots show the overall mean thickness variability, and the error bars indicate one standard deviation. Left: left hemisphere; right: right hemisphere. A smoothing kernel of size  $\sigma = 6$  mm was applied on the raw thickness maps. The scanner upgrade significantly reduces the measurement variability, while the reproducibility error across-scanner upgrade is comparable with that on the old scanner platform.

global mean of the cortical thickness of each subject as measured from each individual scan session. As can be seen, the global mean thickness measure is again highly repeatable, and there is no noticeable bias caused by the scanner upgrade.

Fig. 12 illustrates the average thickness measurement variability and its standard deviation for each hemisphere, computed using repeated scans on the old and new scanner respectively and also for repeated measurements across the scanner upgrade. Detailed maps of the local thickness measurement variability are shown in Fig. 13 (only the left hemisphere is shown; the right hemisphere is similar). From these figures, it can be seen that pooling data across the scanner upgrade does not degrade the measurement reproducibility, and the overall measurement variability across the scanner upgrade stays roughly the same as that on the old scanner platform. It is also

clear that the scanner upgrade significantly reduces the within-scanner measurement variability, which is below 0.1 mm in average for both hemispheres (a smoothing kernel of size  $\sigma = 6$  mm was used). In a separate study (Jovicich et al., 2005), it was found that the scanner upgrade substantially improves the image intensity reproducibility across repeated scans of the same subject, which we believe is the major reason for the much improved thickness measurement reliability.

#### Power analysis

Using the measurement error estimation from the reliability studies, we computed the sample size table shown in Table 2, where we assumed a significance level of 0.05 (one-sided) and a

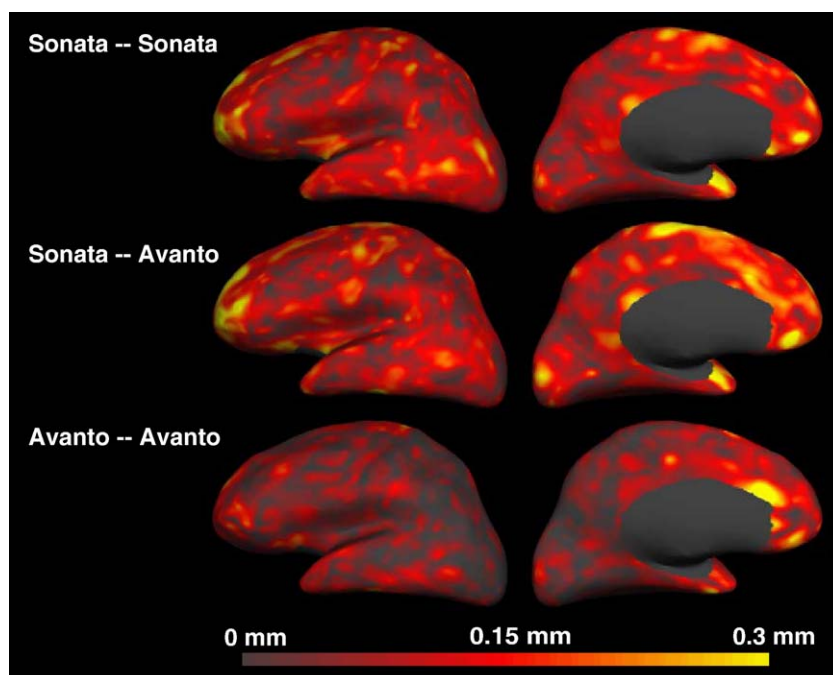


Fig. 13. Maps of thickness measurement variability both before and after the scanner upgrade. Left, lateral view; right: medial view. Only the left hemisphere is shown here; the right hemisphere is similar. A smoothing kernel of size  $\sigma = 6$  mm was applied when generating the thickness difference maps.

Table 2

Calculation of the sample sizes (subjects per group) required to detect (significance level at 0.05, one-sided, statistical power of 0.9) thickness difference effects under various conditions of measurements errors (cf. Figs. 1, 3 and 6)

		Underlying cortical thickness difference effect to be detected (mean thickness = 2 mm)		
		10% <sup>a</sup>	5% <sup>b</sup>	2.5% <sup>c</sup>
Measurement error (STD)	1% <sup>d</sup>	2	2	4
	4.5% <sup>e</sup>	5	15	57
	6% <sup>f</sup>	7	26	100
	7.5% <sup>g</sup>	11	40	155

<sup>a</sup> Approximate effect size for between group differences comparing AD patients to controls.

<sup>b</sup> Approximate effect size for longitudinal comparison of atrophy rates in AD vs. controls.

<sup>c</sup> Approximate effect size for drug that slows rate of atrophy in AD by 50% in 1 year.

<sup>d</sup> Conditions for sample data pooled within scanner, analyzing global mean thickness.

<sup>e</sup> Conditions for sample data pooled within scanner, analyzing local thickness maps, applying longitudinal analysis methods (longitudinal group comparison study).

<sup>f</sup> Conditions for sample data pooled within scanner, analyzing local thickness maps (cross-sectional group comparison study).

<sup>g</sup> Conditions for sample data pooled across scanner and across field strength, analyzing local thickness maps, applying longitudinal analysis methods (multi-center longitudinal clinical drug trial).

statistical power of 0.9. Three scenarios are used to illustrate the application of the techniques used in this paper to clinical neuroscience research. For a study that aims to find group differences in cortical thickness in Alzheimer's disease compared to controls, subjects are typically scanned on the same scanner and data would be analyzed cross-sectionally. The average measurement standard deviation is about 0.12 mm (with a 6 mm spatial smoothing kernel for the thickness maps; cf. Figs. 3 and 6) or 6% of the cortical ribbon (assuming a mean cortical thickness of 2 mm). The computation shows that it requires 7 subjects per group (or 14 subjects in total) to detect a thickness difference of 10% (0.2 mm) (Thompson et al., 2003). For a study that aims to find group differences in the rate of regional cortical atrophy in Alzheimer's disease compared to controls, subjects are typically scanned on the same scanner and data would be analyzed longitudinally. The number of subjects required for this type of study is 15 per group, based on an estimated effect size of 5% (0.1 mm) (Thompson et al., 2003) and a measurement error of 4.5% (0.09 mm; cf. Fig. 6). Finally, for a longitudinal, multi-center clinical drug trial of a compound that aims to slow the rate of atrophy by 50% in 1 year in a group of AD patients compared to a placebo group, subjects would be scanned on different scanners and data would be analyzed longitudinally. The number of subjects required for this type of study is 155 per group, based on an estimated effect size of 2.5% (0.05 mm) and a measurement error of 7.5% (0.15 mm; cf. Fig. 6).

## Conclusion

The purpose of this study is to evaluate the reliability (precision) of an automated thickness measurement method both

within- and across-scanner platforms and field strength. We also evaluated the effects on thickness measurement reliability of different imaging acquisition protocols (including number of acquisitions and imaging sequences) and different data processing or post-processing (smoothing of thickness map) schemes. Finally, we investigated the impact of a scanner upgrade on thickness measurement reproducibility. The results reported in this paper can help the design and assessment of multi-site or longitudinal studies that require accumulating data across multiple scanner platforms or across major scanner upgrades.

Two sets of test–retest scans were acquired and analyzed in this reliability study. From the first data set, within-scanner variability was found to be less than 0.03 mm for global cortical thickness measurement and approximately 0.12 mm in average for local thickness measurement (with a small spatial smoothing of kernel size 6 mm). The variability of local thickness measurements is slightly increased to about 0.15 mm in average across platforms (Siemens and GE) and further increased to 0.17 mm across different field strengths. Although the measurement variability is still low, it was found that thickness measurements across field strength were slightly biased. This measurement bias must be taken into account in the design of multi-site or longitudinal studies that acquire data across field strength, the effect of which could be reduced by balancing subject populations across field strength or by deriving new pulse sequences that can minimize the differences in image contrast under different field strengths.

The results from the second data set allow us to conclude that the thickness measurements were not affected by the scanner upgrade evaluated. In particular, the major upgrade does not increase the measurement variability nor introduce any bias to the thickness measurements. The within-scanner measurement variability, however, can be further reduced when acquiring data only on the newer scanner platform, reflecting the increased SNR and stability afforded by the Siemens Avanto scanner when compared to that of the Sonata system.

Other results showed that between one or two averaged MPRAGE scans there was a negligible effect on thickness measurement reliability, but different data processing or post-smoothing schemes and different imaging sequences can have a large impact on the thickness measurement reproducibility. For example, thickness measurement variability can be substantially reduced by applying smoothing filters on the raw thickness maps. The choice of smoothing kernel size in practice should depend on the estimation of measurement noise and also on the spatial scale or resolution of the thickness change to be found.

Overall, predictions from the test–retest results indicate that a group difference of 0.2 mm (10%) in regional cortical thickness may be reliably identified with as few as 7 subjects per group when using data acquired on the same scanner platform, or as few as 11 subjects per group if using data pooled across multiple scanner platforms. Thus, we can conclude that FreeSurfer is a highly reliable method for automated cortical thickness measurement and may be a useful tool for the investigation of longitudinal brain development, pathophysiological brain changes and the efficacy of clinical interventions.

It should be noted that the study reported in this manuscripts is not a random effects study and the results should not be blindly extrapolated to other pulse sequences and other scanners or scanner types not included in this study.

## Acknowledgments

This research was supported by the following grants: a) NCCR Morphometry Biomedical Informatics Research Network (U24 RR021382), b) NCCR P41-RR14075 and RO1-RR16594-01A1, c) Pfizer Inc., d) the NIA (K23-AG22509 and P01-AG04953) and e) the MIND Institute.

## References

- Barta, P., Miller, M.I., Qiu, A., 2005. A stochastic model for studying the laminar structure of cortex from MRI. *IEEE Trans. Med. Imag.* 24, 728–742.
- Benner, T., Wisco, J.J., van der Kouwe, A., Fischl, B., Vangel, M.G., Hochberg, F.H., Sorensen, A.G., in press. Comparison of manual and automatic slice positioning of brain MR images. *Radiology*.
- Bovee, B.F., Maraganore, D.M., Parisi, J.E., Ahlskog, J., Graff-Radford, N., Caselli, R., Dickson, D., Kokmen, E., Peterson, R., 1999. Pathologic heterogeneity in clinically diagnosed corticobasal degeneration. *Neurology* 53, 795–800.
- Braitenberg, V., Schuz, A., 1991. *Anatomy of the Cortex*. Springer-Verlag, Berlin.
- Chung, M.K., Robbins, S.M., Dalton, K.M., Davidson, R.J., Alexander, A.L., Evans, A.C., 2005. Cortical thickness analysis in autism with heat kernel smoothing. *NeuroImage* 25, 1256–1265.
- Cohen, J., 1988. *Statistical Power Analysis for the Behavioral Sciences*. Lawrence Erlbaum Assoc.
- Dale, A.M., Fischl, B., Sereno, M.I., 1999. Cortical surface-based analysis: I. Segmentation and surface reconstruction. *NeuroImage* 9, 179–194.
- Dickerson, B.C., Sperling, R.A., 2005. Neuroimaging biomarkers for clinical trials of disease-modifying therapies in Alzheimer's disease. *NeuroRx* 2, 348–360.
- Dickerson, B., Goncharova, I., Sullivan, M.P., Forchetti, C., Wilson, R., Bennett, D.A., Beckett, L.A., deToledo-Morrell, L., 2001. MRI-derived entorhinal and hippocampal atrophy in incipient and very mild Alzheimer's disease. *Neurobiol. Aging* 22, 747–754.
- Duda, R.O., Hart, P.E., Stork, D.G., 2001. *Pattern Classification*, 2nd ed. Wiley, New York.
- Fischl, B., Dale, A.M., 2000. Measuring the thickness of the human cerebral cortex from magnetic resonance images. *Proc. Natl. Acad. Sci. U. S. A.* 97, 11050–11055.
- Fischl, B., Sereno, M.I., Dale, A.M., 1999a. Cortical surface-based analysis: II. Inflation, flattening, and a surface-based coordinate system. *NeuroImage* 9, 195–207.
- Fischl, B., Sereno, M.I., Tootell, R.B., Dale, A.M., 1999b. High-resolution intersubject averaging and a coordinate system for the cortical surface. *Hum. Brain Mapp.* 8, 272–284.
- Fischl, B., Liu, A., Dale, A.M., 2001. Automated manifold surgery: constructing geometrically accurate and topologically correct models of the human cerebral cortex. *IEEE Trans. Med. Imag.* 20, 70–80.
- Fischl, B., Salat, D.H., Busa, E., Albert, M., Dieterich, M., Haselgrove, C., van der Kouwe, A., Killiany, R., Kennedy, D., Klaveness, S., Montillo, A., Makris, N., Rosen, B., Dale, A.M., 2002. Whole brain segmentation: automated labeling of neuroanatomical structures in the human brain. *Neuron* 33, 341–355.
- Fischl, B., Salat, D., Van der Kouwe, A., Makris, N., Segonne, F., Quinn, B.T., Dale, A., 2004a. Sequence-independent segmentation of magnetic resonance images. *NeuroImage* 23, 69–84.
- Fischl, B., Van der Kouwe, A., Destrieux, C., Halgren, E., Segonne, F., Salat, D., Busa, E., Seidman, L., Goldstein, J., Kennedy, D., Caviness, V.S., Makris, N., Rosen, B., Dale, A., 2004b. Automatically parcellating the human cerebral cortex. *Cereb. Cortex* 14, 11–22.
- Han, X., Pham, D.L., Tosun, D., Rettmann, M.E., Xu, C., Prince, J.L., 2005a. CRUISE: cortical reconstruction using implicit surface evolution. *NeuroImage* 23, 997–1012.
- Han, X., Jovicich, J., Salat, D., Van der Kouwe, A., Dickerson, B., Quinn, B.T., Rosas, H.D., Makris, N., Dale, A., Fischl, B., 2005b. CNR comparison of three pulse sequences for structural MR brain imaging. *NeuroImage Human Brain Mapping Conference*, Toronto, CA.
- Jack Jr., C.R., Petersen, R.C., Xu, Y.C., Waring, S.C., O'Brien, P.C., Tangalos, E.G., Smith, G.E., Ivnik, R.J., Kokmen, E., 1997. Medial temporal atrophy on MRI in normal aging and very mild Alzheimer's disease. *Neurology* 49, 786–794.
- Jack Jr., C.R., Slomkowski, M., Gracon, S., Hoover, T.M., Felmlee, J.P., Stewart, K., Xu, Y., Shiung, M., O'Brien, P.C., Cha, R., Knopman, D., Peterson, R.C., 2003. MRI as a biomarker of disease progression in a therapeutic trial of milameline for AD. *Neurology* 60, 253–260.
- Jenkinson, M., Bannister, P., Brady, M., Smith, S., 2002. Improved optimization for the robust and accurate linear registration and motion correction of brain images. *NeuroImage* 17, 825–841.
- Jones, S.E., Buchbinder, B.R., Aharon, I., 2000. Three-dimensional mapping of cortical thickness using Laplacian's equation. *Hum. Brain Mapp.* 11, 12–32.
- Joshi, M., Cui, J., Doolittle, K., Joshi, S., Essen, D., Wang, L., Miller, M.L., 1999. Brain segmentation and the generation of cortical surfaces. *NeuroImage* 9, 461–476.
- Jovicich, J., Czanner, S., Greve, D.N., Pacheco, J., Busa, E., Van der Kouwe, A., Morphometry, B.I.R.N., Fischl, B., 2005. Test–retest reliability reproducibility assessments for longitudinal studies: quantifying MRI system upgrade effects. *ISMRM Scientific Meeting*. Miami, FL.
- Kiernan, J.A., Hudson, A.J., 1994. Frontal lobe atrophy in motor neuron diseases. *Brain* 117, 747–757.
- Kuperberg, G.R., Broome, M., McGuire, P.K., David, A.S., Eddy, M., Ozawa, F., Goff, D., West, W.C., Williams, S.C.R., Van der Kouwe, A., Salat, D., Dale, A., Fischl, B., 2003. Regionally localized thinning of the cerebral cortex in schizophrenia. *Arch. Gen. Psychiatry* 60, 878–888.
- Lerch, J.P., Evans, A.C., 2005. Cortical thickness analysis examined through power analysis and a population simulation. *NeuroImage* 24, 163–173.
- Lerch, J.P., Pruessner, J.C., Zijdenbos, A., Hampel, H., Teipel, S.J., Evans, A.C., 2005. Focal decline of cortical thickness in Alzheimer's disease identified by computational neuroanatomy. *Cereb. Cortex* 15, 955–1001.
- MacDonald, D., Kabani, N., Avis, D., Evans, A.C., 1999. Automated 3-D extraction of inner and outer surfaces of cerebral cortex from MRI. *NeuroImage* 12, 340–356.
- Narr, K.L., Bilder, R.M., Toga, A.W., Woods, R.P., R.D., E., Szeszko, P.R., Robinson, D., Sevy, S., Gunduz-Bruce, H., Wang, Y.-P., Deluca, H., Thompson, P., 2005. Mapping cortical thickness and gray matter concentration in first episode schizophrenia. *Cereb. Cortex* 15, 708–719.
- Rosas, H.D., Liu, A.K., Hersch, S., Glessner, M., Ferrante, R.J., Salat, D.H., van der Kouwe, A., Jenkins, B.G., Dale, A.M., Fischl, B., 2002. Regional and progressive thinning of the cortical ribbon in Huntington's disease. *Neurology* 58, 695–701.
- Sailer, M., Fischl, B., Salat, D., Tempelmann, C., Schonfeld, M., Busa, E., Bodammer, N., Heinze, H., Dale, A., in press. Focal thinning of the cerebral cortex in multiple sclerosis. *Brain*.
- Salat, D.H., Kaye, J.A., Janowsky, J.S., 1999. Prefrontal gray and white matter volumes in healthy aging and Alzheimer disease. *Arch. Neurol.* 56, 338–344.
- Salat, D., Buckner, R.L., Snyder, A.Z., Greve, D.N., Desikan, R.S., Busa, E., Morris, J.C., Dale, A., Fischl, B., 2004. Thinning of the cerebral cortex in aging. *Cereb. Cortex* 14, 721–730.
- Segonne, F., Dale, A., Busa, E., Glessner, M., Salat, D., Hahn, H.K., Fischl, B., 2004. A hybrid approach to the skull stripping problem in MRI. *NeuroImage* 22, 1060–1075.
- Shattuck, D.W., Leahy, R.M., 2002. BrainSuite: an automated cortical surface identification tool. *Med. Image Anal.* 6, 129–142.
- Sowell, E.R., Peterson, B.S., Thompson, P., Welcome, S.E., Henkenius,

- A.L., Toga, A.W., 2003. Mapping cortical changes across the human life span. *Nat. Neurosci.* 6, 309–315.
- Sowell, E.R., Thompson, P., Leonard, C.M., Welcome, S.E., Kan, E., Toga, A.W., 2004. Longitudinal mapping of cortical thickness and brain growth in normal children. *J. Neurosci.* 24, 8223–8231.
- Steen, R.G., Reddick, W.E., Ogg, R.J., 2000. More than meets the eye: significant regional heterogeneity in human cortical T1. *Magn. Reson. Imaging* 18, 361–368.
- Thompson, P., Vidal, C.N., Giedd, J.N., Gochman, P., Blumenthal, J., Nicolson, R., Toga, A.W., Rapoport, J.L., 2001. Mapping adolescent brain change reveals dynamic wave of accelerated gray matter loss in very early onset schizophrenia. *Proc. Natl. Acad. Sci. U. S. A.* 98, 11650–11655.
- Thompson, P., Hayashi, K.M., Zubicaray, G., Janke, A.L., Rose, S.E., Semple, J., Herman, D., Hong, M.S., Dittmer, S.S., Doddrell, D.M., Toga, A.W., 2003. Dynamics of gray matter loss in Alzheimer's disease. *J. Neurosci.* 23, 994–1005.
- Van der Kouwe, A., Benner, T., Fischl, B., Schmitt, F., Salat, D., Harder, M., Sorensen, A.G., Dale, A., 2005. On-line automatic slice positioning for brain MR imaging. *NeuroImage* 27, 222–230.
- van Essen, D.C., Dickson, J., Harwell, J., Hanlon, D., Anderson, C.H., Drury, H.A., 2001. An integrated software system for surface-based analyses of cerebral cortex. *J. Am. Med. Inform. Assoc.* 8, 443–459.
- Walters, R.J.C., Fox, N.C., Crum, W.R., Taube, D., Thomas, D.J., 2001. Hemodialysis and cerebral edema. *Nephron* 87, 143–147.
- Xu, C., Pham, D.L., Rettmann, M.E., Yu, D.N., Prince, J.L., 1999. Reconstruction of the human cerebral cortex from magnetic resonance images. *IEEE Trans. Med. Imag.* 18, 467–480.
- Yezzi, A., Prince, J.L., 2003. An Eulerian PDE approach for computing tissue thickness. *IEEE Trans. Med. Imag.* 22, 1332–1339.
- Zeng, X., Staib, L.H., Schultz, R.T., Duncan, J.S., 1999. Segmentation and measurement of the cortex from 3D MR images using coupled surfaces propagation. *IEEE Trans. Med. Imag.* 18, 100–111.